Journal of Molecular and Cellular Cardiology Plus 3 (2023) 100030

Contents lists available at ScienceDirect

Journal of Molecular and Cellular Cardiology Plus

journal homepage: https://www.journals.elsevier.com/journal-of-molecular-and-cellular-cardiology-plus

Myocardial overexpression of protein phosphatase 2A-B56α improves resistance against ischemia-reperfusion injury

Julius R. Herting [a,*], Anna M. Berg [b], Katarina Hadova [a,d], Alexander Heinick [a], Simone König [b], Michael Kuhlmann [c], Frank U. Müller [a], Uwe Kirchhefer [a]

[a] Institut für Pharmakologie und Toxikologie, Westfälische Wilhelms-Universität Münster, Domagkstr. 12, 48149 Münster, Germany
[b] Interdisziplinäres Zentrum für Klinische Forschung, Integrierte Funktionelle Genomik, Westfälische Wilhelms-Universität Münster, Röntgenstraße 21, 48149 Münster, Germany
[c] European Institute for Molecular Imaging, Universitätsklinikum Münster, Waldeyerstr. 15, 48149 Münster, Germany
[d] Department of Pharmacology and Toxicology, Faculty of Pharmacy, Comenius University, Bratislava, Slovakia

ARTICLE INFO

Keywords:
Protein phosphatase 2A
Ischemia-reperfusion
Contractility
Protein phosphorylation
RISK signaling pathway
Acidosis
LAD
Fibrosis

ABSTRACT

Protein phosphatase 2A (PP2A) plays a central role in myocardial ischemia-reperfusion (I/R) injury. Several studies showed a detrimental function of PP2A by using either overexpression models of the catalytic subunit (PP2Ac) or exogenous inhibitors of PP2Ac. However, all of these approaches underestimate the contribution of regulatory B subunits in modulating the PP2A holoenzyme. To better understand the influence of B subunits on a "controlled" regulation of PP2A, we tested a mouse model overexpressing PP2A-B56α (TG) in the heart under the conditions of I/R in comparison to wild-type littermates (WT). Contractility was increased after reperfusion in isolated TG hearts that were initially subjected to a 20-min no-flow ischemia. This was associated with lower phosphorylation levels of myosin-binding protein C and the ryanodine receptor 2 in TG compared to WT. The application of okadaic acid abolished the contractile and biochemical effects in TG hearts. Moreover, reperfusion resulted in the detection of higher PP2A-B56α levels in mitochondrial preparations of TG hearts. The phosphorylation of ERK1 was increased in the early reperfusion phase in TG compared to WT hearts corresponding to a transient attenuation of PP2A activity. Ischemia led to a prolonged contracture time in TG hearts and a lower acidification in isolated TG cardiomyocytes. The formation of interstitial fibrosis by transient ligation of the left anterior descending (LAD) artery was reduced in TG compared to WT hearts. Taken together, these findings indicate that overexpression of PP2A-B56α is protective against I/R injury and that B56α merits further investigation as a potential therapeutic target.

1. Introduction

Myocardial ischemia is a major cause of morbidity and mortality worldwide. It is well known that myocardial ischemia results in reduction or loss of contractility and tissue damage as a result of cardiomyocyte death [1]. Prompt reperfusion of the ischemic heart restores coronary flow, supply of oxygen and nutrients and finally cardiac contractile function leading to the rescue of myocardium and patient survival [2]. However, paradoxically reperfusion results also in inflammatory reactions and oxidative stress leading to cell death and irreversible myocardial injury. This process is called ischemia-reperfusion (I/R) injury.

Over the past two decades, much work has been devoted to identifying the cellular mechanisms that both contribute to ischemia and/or reperfusion damage and protect against it [3,4]. It is now widely accepted that phosphorylation levels of cardiac Ca^{2+} regulatory proteins play a critical role in determining the extent of myocardial I/R injury [5]. Reversible protein dephosphorylation is thereby exerted by serine/threonine protein phosphatases (PP's). Studies at the end of the last century already demonstrated that protein phosphatase 2A (PP2A) significantly contributes to the myocellular regulation of ischemia and I/R. This was demonstrated by the use of naturally occurring and synthetic inhibitors of the catalytic subunit (PP2Ac). For example, calyculin A and okadaic acid were able to reduce the anoxic and ischemic injury in isolated rat cardiomyocytes [6]. In line with these findings, fostriecin, also an inhibitor of PP2A, protected the rabbit heart from infarction [7]. Both studies suggest that higher levels of PP2Ac contribute to the development of irreversible myocardial cell injury. Consistently, PP2Ac-overexpressing mice developed hypertrophy and fibrosis of the remote myocardial infarct site after chronic myocardial infarction by ligation of the left anterior descending (LAD) artery [8]. These findings were associated with restoration of the disrupted basal Akt/glycogen synthase kinase (GSK)-3β/β-catenin signaling in transgenic mice. Surprisingly, despite the negative effects of increased PP2A activity the survival of transgenic mice was even improved in the chronic phase after myocardial infarction suggesting even protective effects of PP2A. All studies mentioned so far aimed to directly alter PP2A activity. However, a large number of studies also exist that mimic cardiac ischemia or I/R by different interventions which were associated with a higher PP2A activity

* Corresponding author.
E-mail address: j_hert04@uni-muenster.de (J.R. Herting).

http://dx.doi.org/10.1016/j.jmccpl.2022.100030
Received 15 December 2022; Accepted 20 December 2022

and/or expression [9,10]. In contrast, in a rat heart I/R model PP2A activity was decreased which was associated with higher phosphorylation levels of Akt, ERK1/2 and GSK3β [11]. A reduced PP2A activity was also detected in an isolated heart model of I/R [12].

The somewhat ambiguous results on PP2A activity/expression in both ischemia studies and I/R models may arise from the fact that samples were analyzed on different time points, that various intervention models were used and that only global cellular effects on PP2Ac were considered. It is therefore difficult to deduce from these experiments whether an altered PP2A activity per se leads to I/R damage or may only represent the attempt to maintain normal myocardial function. This requires a more detailed view on the local regulation of PP2Ac in myocardial tissue. This, in turn, is controlled by regulatory B subunits that provide substrate specificity and subcellular targeting [13,14] forming together with PP2Ac and a scaffolding A subunit an active heterotrimer. The B′ subfamily is the largest B subfamily with five members and is preferentially expressed in the heart [15,16] of which B56α in turn shows the highest expression in the heart [13,17,18]. It has been shown by our group that B56α was able to inhibit the PP2A [19]. In addition, transgenic mice with heart-directed overexpression of PP2A-B56α exhibited concomitantly higher PP2Ac expression levels and PP2A activity. This aspect was linked to a target-specific dephosphorylation of myofilament proteins resulting in increased Ca^{2+} sensitivity and higher contractility [20].

Therefore, the present study was undertaken to test whether the positive contractile effects shown in our previously characterized PP2A-B56α overexpression model can be transferred to a potential protection against I/R injury. For this purpose, functional effects were measured in the whole animal after transient LAD ligation, in isolated hearts with global ischemia and subsequent reperfusion, and in individual cardiomyocytes with ischemia simulation.

2. Materials and methods

2.1. Experimental animals

Generation of transgenic FVB/N mice with overexpression of PP2A-B56α (TG) [20] was previously described. TG and wild-type (WT) littermates were used at 20–24 weeks of age. Mice were kept at room temperature under a 12 h light/dark cycle and received normal diet (Altromin) and water ad libitum. The mice were euthanized with CO_2. All procedures were conducted in accordance with local animal welfare authorities and approved by the LANUV, Germany (Ref. no. 84_02.04.2014.A485).

2.2. Langendorff-perfused hearts

Heart preparations were obtained as described previously [20]. Mice were anesthetized intraperitoneally with 2.0 g/kg body weight urethane and treated with 1.5 units of heparin. Hearts were removed from the opened chest, immediately attached by the aorta to a 20-gauge cannula, and perfused retrogradely under constant pressure of 50 mm Hg with oxygenized Krebs-Henseleit buffer (37.4 °C) in an isolated heart system (Hugo Sachs Elektronik). The heart preparations were allowed to equilibrate for 30 min before starting measurements. The hearts were stimulated at 8 Hz and heart rate, aortic pressure, and LV pressure were measured and monitored continuously. The first derivative of LV pressure (+dP/dt and -dP/dt) and the time to ischemic contracture were calculated (ISOHEART Software, Hugo Sachs Elektronik). To generate global ischemia, the perfusion was stopped for 20 min and thereafter the hearts were reperfused for 40 min. Where indicated, 3 nM okadaic acid was added to the perfusion buffer to block completely PP2A activity.

2.3. Isolation of mouse cardiomyocytes

Cardiomyocytes were isolated from mice by enzymatic digestion [21]. Briefly, excised hearts were rinsed with heparin and retrogradely perfused with collagenase solution (collagenase type II; Worthington Biochemical, Lakewood, NJ, USA) in a modified Langendorff apparatus (37 °C, 2 ml/min). The cells were then separated by mechanical dispersion and Ca^{2+} concentration was progressively increased to 1 mM before initiating the experiments.

2.4. Preparation of mitochondria from isolated hearts

Mitochondria-enriched samples were isolated from Langendorff-perfused hearts by differential centrifugation using a modified protocol [22]. Briefly, hearts were washed in ice-cold isolation buffer (225 mM mannitol, 75 mM sucrose, 10 mM Hepes, 10 mM Tris, and 1 mM EGTA, pH = 7.4 adjusted with Tris), and 1-mm^3 pieces were homogenized in the isolation buffer, supplemented with 0.1 mg/ml Nagarse (Sigma-Aldrich), using a glass-Teflon homogenizer. 6 ml of isolation buffer, in which bovine serum albumin (0.2 %) was dissolved, were added and samples were centrifuged at 500 × *g* for 10 min (at 4 °C). Thereafter, the supernatant was filtered through a 150-μm mesh and centrifuged again at 10,000 ×*g* for 10 min. The pellet was resuspended in the isolation buffer (with added 0.2 % BSA) and spun at 7500 ×*g* for 6 min. The pellet was washed with the isolation buffer and centrifuged at 7500 ×*g* for 6 min. Finally, the mitochondria-enriched pellet was resuspended in the isolation buffer and stored at − 80 °C. Protein concentration was determined based on the Bradford method utilizing Bio-Rad protein assay kit (Bio-Rad).

2.5. Protein phosphatase assay

Protein phosphatase activity was measured as previously described [23]. Mouse ventricular tissue was homogenized by sonification at 4 °C for 1 min in buffer containing 4 mM EDTA (pH = 7.4) and 15 mM 2-mercaptoethanol. Homogenates were centrifuged at 14,000 × *g* for 20 min at 4 °C, and supernatants were used for determination of phosphorylase phosphatase activity. The reaction mixture contained 20 mM Tris/HCl (pH = 7.4), 5 mM caffeine, 0.1 mM EDTA, and 15 mM 2-mercaptoethanol. Dephosphorylation was initiated by adding ^{32}P-phosphorylase *a* to a final concentration of 0.5 mg/ml (40,000 cpm/nmol) and carried out at 30 °C for 10 min in the absence and presence of 3 nM okadaic acid. The reaction was terminated by addition of 50 % trichloroacetic acid. Precipitated proteins were sedimented at 10,000 × *g* and an aliquot of the supernatants was counted in a liquid scintillation counter (Packard Tri-Carb).

2.6. SDS-PAGE and immunoblotting

Homogenates were prepared from mitochondrial preparations or from frozen pulverized heart tissue powder that was suspended in 10 mM $NaHCO_3$ solution supplemented with a protease and phosphatase inhibitor cocktail (Roche). The mixture was homogenized with three 10-s pulses using ultrasound (HTU Soni 130). Then, proteins were denatured in 5 % SDS and incubated at room temperature for 20 min. After a centrifugation at 14,000 × *g* for 20 min, supernatants were removed for subsequent determination of protein concentration and analysis of protein expression. Depending on the protein to be analyzed, a volume equivalent to 100 or 200 μg of protein was taken from the supernatants that were supplemented with an equal volume of 2×-Laemmli buffer. Samples were boiled for 10 min and then subjected to SDS polyacrylamide gel electrophoresis. Thereafter, separated proteins were transferred to nitrocellulose membranes. Blots were incubated with specific antibodies raised against the following proteins: B56α of PP2A (1:1000, Bethyl), Akt (1:1000, Santa Cruz), Akt pSer^{473} (1:1000, Cell Signaling), ERK1/2 (1:1000, Fitzgerald), pERK1/2 (1:1000, BioLegend), cTnI (1:1000, Cell Signaling), cTnI pSer$^{23/24}$ (1:1000, Cell Signaling), cMyBP-C (1:1000, LSBio), cMyBP-C pSer^{282} (1:1000, Enzo), MLC2 (1:1000, Cell Signaling), MLC2 pSer^{18} (1:1000, Origene), RyR2 (1:1000) [24], RyR2 pSer^{2808} (1:1000, Badrilla), VDAC1 (1:2000, Abcam). The amounts of bound antibodies were detected by use of secondary antibodies (ECL rabbit/goat IgG, HRP-linked whole Ab, GE Healthcare). Signals were visualized and quantified with the ECL plus

detection system (Amersham ECL Plus, GE Healthcare) and the ChemiDoc XRS system, respectively. All antibodies used have been applied several times in previous studies where they were already established. Phospho-antibody adjustment was performed on the protein to be determined. A control sample was loaded on each blot to control for normal variation between blots. The individual samples were adjusted to this control sample.

2.7. Measurement pH resistance (pHrodo Red AM)

Isolated ventricular cardiomyocytes were placed into an incubation chamber on Laminin-coated coverslips. 1 μl of pHrodo Red AM (ThermoFisher Scientific) was mixed with 10 μl of PowerLoad concentrate and then diluted in 989 μl Krebs-Henseleit buffer. Cardiomyocytes were incubated in this mix at room temperature for 30 min. Cells were then washed for 5 min with Krebs-Henseleit buffer gassed with carbogen (5 % CO_2 and 95 % O_2). Perfusion was changed to mixed gas (20 % CO_2) for 30 min. Fluorescence was recorded with an LSM 710 confocal fluorescence microscope (Zeiss) with excitation at 543 nm. Emission was detected through 555–597 nm bandpass filters. ZEN blue software (Zeiss) was used to define regions of interest and F_1/F_0 was calculated continuously.

2.8. 2D differential gel electrophoresis and mass spectrometry

Tissue (30 mg ± 5 mg) was homogenized in 1 ml lysis buffer (7 M urea, 2 M thiourea, 2 % CHAPS, 65 mM DTT, 2 % Bio-Lyte 3/10 (40 %, Bio-Rad)) using the Labsonic M (Sartorius) ultrasonic device with a 2.0 mm diameter probe. The homogenates were centrifuged at 30,000 ×*g* for 15 min at 4 °C, and 700 μl of each supernatant was transferred into a new vial. The protein concentration was determined with the Advanced Protein Assay Reagent (ADV01-A, Cytoskeleton).

Differential two-dimensional gel electrophoresis (2D) was performed using the HPE Flat Top Tower (SERVA) and pre-cast 2D HPE large format gels (2DHPE™ Large Gel NF 12.5 %; size 255 × 200 × 0.65 mm). All reagents and material were from SERVA if not otherwise noted. For isoelectric focusing, 24 cm IPG BlueStrips pH 3-10 L were passively rehydrated with 450 μl rehydration buffer (8 M urea, 1 % CHAPS, 13 mM DTT, 0.5 % SERVALYTE 3-10 (40 %), 0.004 % (w/v) bromophenol blue) without sample at room temperature overnight. Per strip, 500 μg of sample was applied via cup-loading at the anodic end. Focusing was performed with an Ettan IPGphor II (GE) using the following program: 3 h at 150 V and 3 h at 300 V, then the voltage was gradually increasing to 1000 V within 6 h and to 8000 V within 4 h. At the end it was held for 3 h at 8000 V. Subsequently, each strip was first equilibrated for 15 min at room temperature and 50 rpm in 6 ml IPG-strip equilibration buffer containing 6 M urea and 1 % DTT and then for 15 min in 6 ml IPG-strip equilibration buffer containing 6 M urea and 2.5 % (w/v) iodoacetamide. The second dimension was performed with the HPE Flat Top Tower as suggested by the manufacturer. Electrode wicks were soaked for 30 min in 50 ml of the ready-to-use electrode buffers included in the 2DHPE™ Large Gel NF 12.5 % Kit. Four pre-cast 2D HPE large format gels were run at the same time. Afterwards, each gel was stained with ProQ-Diamond phosphoprotein gel stain (Life Technologies) according to the manufacturer's instructions using half of the recommended volumes. Briefly, gels were fixated in 250 ml fixation solution for 30 min at room temperature using a horizontal shaker (50 rpm). With fresh 250 ml fixation solution fixation continued overnight. Subsequently, gels were washed three times in 250 ml MilliQ-water (15 min, 50 rpm). Gels were then placed in 250 ml Pro-Q Diamond phosphoprotein gel stain and stained on a horizontal shaker (2 h, room temperature, 50 rpm). Afterwards, the staining solution was replaced by 250 ml destaining solution and destained thrice (30 min each, 50 rpm). Gels were washed in 250 ml MilliQ-water twice (5 min, 50 rpm). Stained gels were scanned with Typhoon 9400 (GE). Gel differential analysis of TG and WT samples (n = 4 each) and spot quantification was performed with the Delta 2D software (DECODON). Spots that differed significantly ($P \leq 0.05$) >1.5-fold in intensity between groups were selected for further analysis.

For protein identification, one of the gels was stained with Quick Coomassie Stain (SERVA) according to the manufacturer's instruction, scanned, and matched to the corresponding ProQ-Diamond stain gel image. A pick list was generated and sent to Ettan Spot Picker (GE), which extracted the chosen spots. These were destained, washed, and tryptically digested in the gel. Peptides were extracted and subjected to nano-reversed-phase chromatography coupled to high-resolution mass spectrometry using nanoAcquity coupled to Q-TOF Premier (Waters Corp.) as described [25] in data-dependent mode. Data analysis was performed with ProteinLynx Global Server 2.3 (Waters Corp.) and the 2013 release of the in-house Mascot server (MatrixScience Ltd.) with the *Mus musculus* Uniprot database (download March 2009). Methionine oxidation was set as flexible and carbamidomethylation as fixed modification allowing one missed cleavage. The mass tolerance was 30 ppm for precursor and 50 ppm for fragment ions. Results were manually evaluated for spectral quality.

2.9. Induction of myocardial infarction

Mice were anesthetized by a combination of injection anesthesia (0.04 mg fentanyl/4 mg midazolam/kg body weight) and by inhalation anesthesia (isofluorane 1.5–2.5 % v/v in O_2) for surgical procedures. Myocardial infarction was induced by transient ligation of the left anterior descending artery (LAD) as previously described [26]. In brief, animals were intubated orotracheally and mechanically ventilated. A left thoracotomy was performed in the fourth intercostal space, the pericardium opened, and the LAD ligated with 7.0 nylon suture with a small plastic tubing inserted in the thread loop. The tubing was removed after 120 min which stopped vessel compression, leading to reperfusion of the LAD. Finally, the thorax, subcutaneous tissue and skin were closed in separate layers by a surgical thread (6.0), and animals were weaned from the ventilator as soon as they started rebreathing during awakening. Postsurgical analgesia was performed by repeated subcutaneous application of buprenorphine (0.1 mg/kg body weight) for at least 24 h after surgery. Mice were killed after a 3-week recovery period by whole-body perfusion and fixation with paraformaldehyde (4 %) in phosphate-buffered saline under deep anesthesia. Hearts then were excised, weighed, and embedded in paraffin for histology.

2.10. Histological examination of fibrosis

Paraffin-embedded hearts were cut into 5-μm serial short-axis sections from apex to base, whereby collecting every 4th and 5th cut (~400 sections per heart). Subsequently, sections were deparaffinized, rehydrated, and subjected to Heidenhain's AZAN trichrome staining which colorizes connective tissue such as the infarct scar deep blue, in contrast to the red cardiomyocytes of the remote heart tissue appearing brick red. For analysis of fibrosis in the sections, the software Image Pro Analyzer 7.0 (Media Cybernetics) was used.

2.11. Data analysis

Data are shown as means ± SD (scatter dot plots with bar) or SE (2-D line plots). Data points represent individual hearts (“N”) or individual cardiomyocytes per heart (“n”). The statistical analysis was performed using the SigmaPlot software (Systat Software GmbH). Depending on the research question and the comparison groups, various statistical tests were used. If the calculation resulted in a P value <0.05, differences between groups were considered significant. Tests and significances are noted in the figure legends.

3. Results

3.1. Improved contractility in the late phase of reperfusion in TG hearts

Several studies on the effects of PP2A on the cellular damage and cardiac remodeling after ischemia report inconsistent findings. Therefore, we

first aimed to test the contractile effects of cardiac-specific overexpression of PP2A-B56α in isolated, Langendorff-perfused hearts that were subjected to a 20-min global no-flow ischemia followed by a 40-min reperfusion period. Both the maximum intraventricular pressure P_{max} (Fig. 1A) and the maximum rate of left ventricular pressure development (Fig. 1B) were increased after 20 min of reperfusion in TG compared to corresponding WT hearts. The application of 3 nM okadaic acid abolished completely the increase in contractility, indicating a PP2A-specific effect. The maximum rate of left ventricular pressure decline was only transiently increased in TG compared to corresponding WT (Fig. 1C). However, this effect was also sensitive to an inhibition of PP2A activity by okadaic acid resulting in a comparable relaxation. The time of ischemic contracture is regarded as an important parameter that reflects the myocardial energy consumption of the heart during phases of ischemia. Here we measured the time when left ventricular diastolic pressure reached 30 mm Hg during global ischemia. The time of ischemic contracture was prolonged by 25 % in TG compared to corresponding WT hearts (Fig. 2A & C). The inhibition of PP2A activity by okadaic acid was associated with a comparable time of ischemic contracture between both groups (Fig. 2B & C), supporting the specificity of the contractile functional phenotype of the PP2A-B56α overexpression model.

3.2. Reduced phosphorylation levels of cardiac regulatory proteins after 40 min of reperfusion in TG hearts

Next, we analyzed whether the improved contractile effects in reperfused TG hearts were associated with concomitant changes in the phosphorylation level of force-generating and/or Ca^{2+} cycling proteins. To this end, we performed immunoblotting experiments on homogenates from samples of Langendorff-perfused hearts after 40 min of reperfusion in the presence and absence of 3 nM okadaic acid. Protein phosphorylation of myosin-binding protein-C (MyBP-C) was reduced by 33 % in TG compared to corresponding WT hearts (Fig. 3A). When okadaic acid was added to the perfusion solution there was no difference anymore between both groups. In contrast, the protein phosphorylation of both the myosin light chain-2 (Fig. 3B) and the troponin inhibitor (Fig. 3C) was not different between TG and WT hearts whether measured in the absence nor in the presence of the PP2A inhibitor. Besides these myofilament proteins, we detected the phosphorylation level of the cardiac ryanodine receptor (RyR2), representing the Ca^{2+} release channel of the junctional sarcoplasmic reticulum. Its phosphorylation level was decreased by 27 % in TG compared to

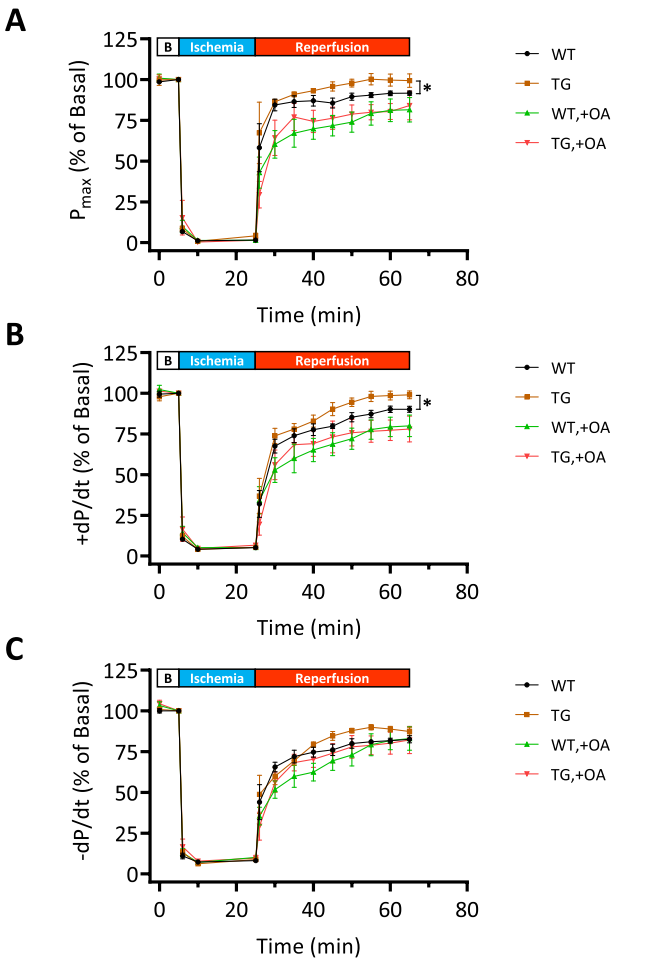

Fig. 1. Improved left ventricular pressure development in TG after ischemia. Isolated, Langendorff-perfused hearts of WT and TG mice were equilibrated (B = basal) and then subjected to a 20-min global no-flow ischemia that was followed by a 40-min reperfusion period. The maximum left ventricular (LV) pressure (A), the maximum rate of LV pressure development (B) and the maximum rate of LV pressure decline (C) were constantly monitored in the absence and presence of 3 nM okadaic acid (± OA) (*$P < 0.05$ vs. WT; two-way ANOVA RM with Holm-Sidak's posttest; N = 5 hearts each group).

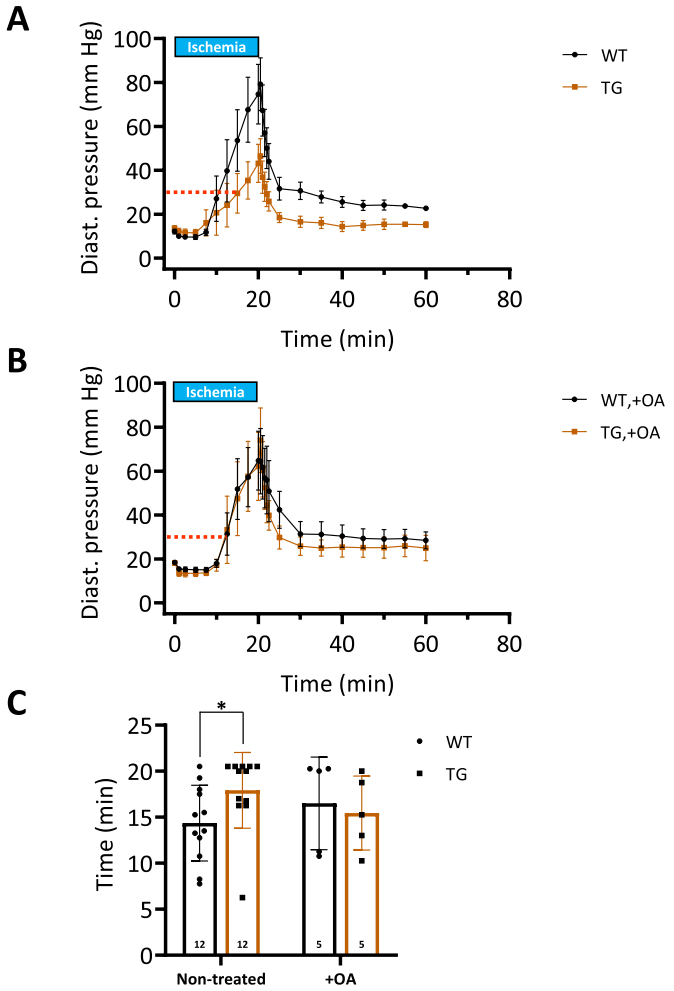

Fig. 2. Attenuated ischemic contracture in TG hearts. Isolated, Langendorff-perfused hearts of both genotypes were equilibrated and then subjected to a 20-min global non-flow ischemia that was followed by a 40-min reperfusion. The maximum diastolic left ventricular pressure was measured in the absence (A) and presence (B) of 3 nM okadaic acid (+OA) (N = 5 hearts each group). The time of ischemic contracture (C) was detected when the diastolic pressure reached 30 mm Hg (red dotted line) (*$P < 0.05$ vs. non-treated WT; unpaired Student's *t*-test; N = 5–12 hearts).

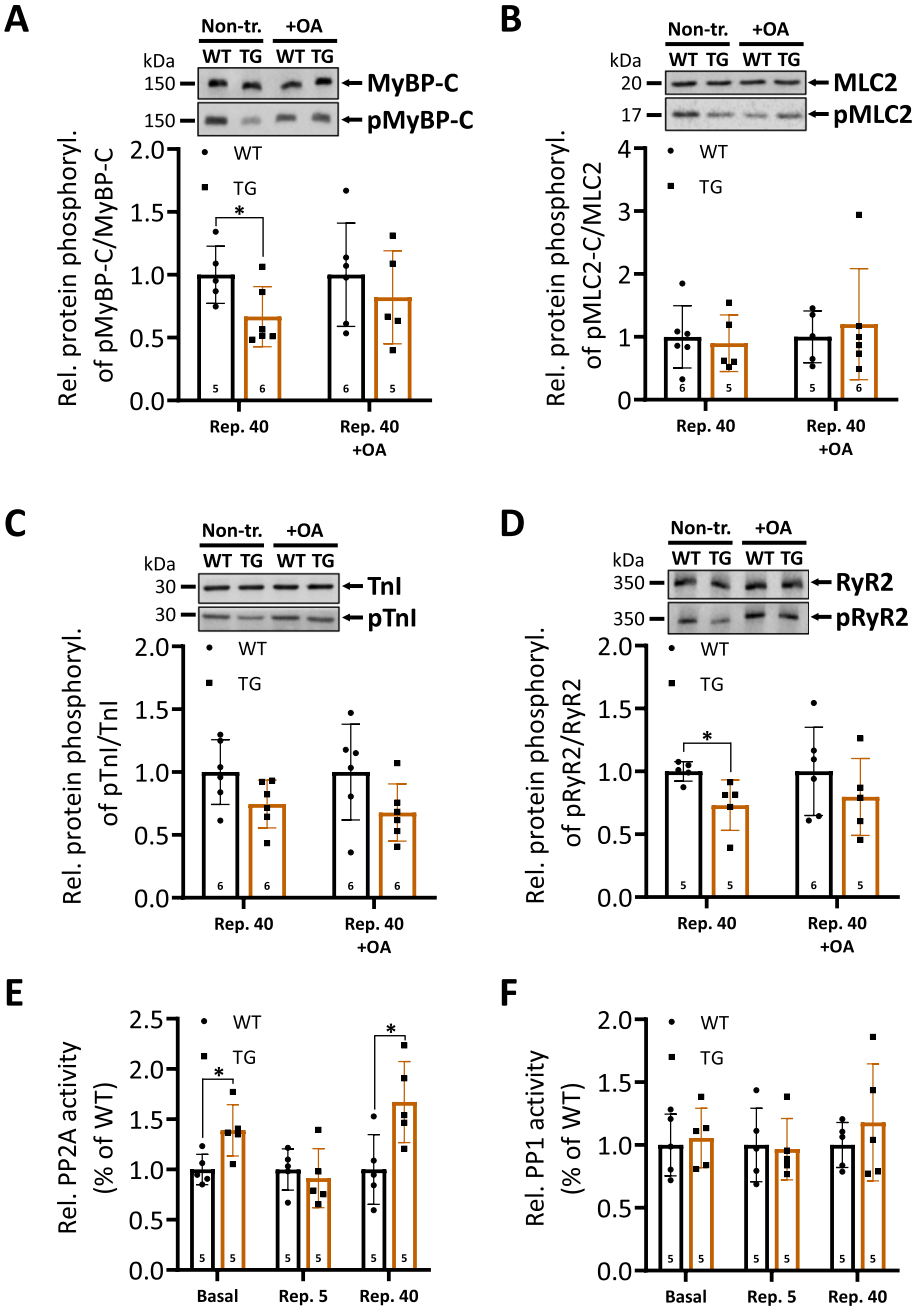

Fig. 3. Reduced phosphorylation of cardiac regulatory proteins in TG hearts in late reperfusion. Isolated, Langendorff-perfused hearts of WT and TG mice were equilibrated and then subjected to a 20-min global non-flow ischemia that was followed by reperfusion. Hearts were analyzed for relative protein phosphorylation 40 min after reperfusion in the absence (non-treated) and presence (+ OA) of 3 nM okadaic acid. The following phosphoproteins were detected: MyBP-C, myosin-binding protein C (A), MLC2, myosin light chain type 2 (B), TnI, troponin inhibitor (C), RyR2, ryanodine receptor type 2 (D). The levels of phosphoproteins were related to the expression of total proteins. Shown are representative immunoblots of non-phosphorylated and phosphorylated proteins (*$P < 0.05$ vs. WT; unpaired Student's *t*-test; N = 5–6 hearts). Protein phosphatase activity was measured in homogenates of hearts sampled under basal conditions, 5 min and 40 min after reperfusion. 3 nM okadaic acid was used to discriminate between type 2A (E) and type 1 (F) phosphatase activities (*$P < 0.05$ vs. WT; one-way ANOVA with Student-Newman-Keuls posttest; N = 5 hearts each group). More original examples of immunoblots are provided in Supplemental Fig. 1.

corresponding WT hearts (Fig. 3D). The application of okadaic acid abolished the decrease in phosphorylation. The levels of non-phosphorylated proteins were unchanged between TG and WT (Fig. 3). Of note, the lower phosphorylation levels of MyBP-C and RyR2 after 40 min of reperfusion fit well with a higher PP2A activity in TG heart homogenates at the corresponding time (Fig. 3E). A higher PP2A activity was also observed at basal conditions before global ischemia was started. In contrast, PP1 activity remained unchanged between both groups (Fig. 3F), suggesting an exclusivity of PP2A-B56α to the altered phosphorylation data.

3.3. Activation of ERK1 in the early phase of reperfusion in TG hearts

To further assess the contribution of the RISK pathway, a vital signaling pathway associated with I/R injury, to the improved contractility in TG hearts, we investigated the phosphorylation levels of AKT and ERK1/2 at different time points. We detected an increased phosphorylation of ERK1 after 5 min of reperfusion in TG compared to corresponding WT heart homogenates (by 182 %), whereas phosphorylation levels of both AKT (Fig. 4A) and ERK1/2 (Fig. 4B & C) were not different between both groups at basal conditions. The levels of non-phosphorylated proteins were not

different between both groups (Fig. 4). Consistent with the time-dependent changes in ERK1 phosphorylation the PP2A activity was attenuated in TG hearts after 5 min of reperfusion compared to basal conditions resulting overall in comparable activity values between both genotypes (Fig. 3E). The recovery of higher PP2A activity in TG hearts after 40 min of reperfusion is paralleled by normalized ERK1 phosphorylation levels (Fig. 4B). A higher phosphorylation was also observed for ERK2 in TG but did not reach statistical significance (Fig. 4C).

3.4. Delayed acidification during ischemia in TG cardiomyocytes

Since the development and progression of I/R injury depend not only on the activation of pro-survival protein kinases during reperfusion but also on metabolic conditions during ischemia, we tested the progression of the intracellular pH value. For this purpose, we loaded isolated cardiomyocytes with the pH-sensitive dye pHrodo Red/AM under conditions of a simulated ischemia by perfusion of cells with 20 % carbon dioxide. At neutral pH (=7.4) the dye showed a low fluorescence signal while it showed a brighter fluorescence with decreasing pH in more acidic environments (Fig. 5A). This acidification results from the hypoxia under perfusion with carbon dioxide, which switches cell metabolism to anaerobic glycolysis and lactate production. Surprisingly, the maximal intracellular acidic pH was reached later in TG compared to corresponding WT cardiomyocytes (Fig. 5B) reflected by a slower rise in the fluorescence signal F_1/F_0. The time to 50 % increase in F_1/F_0 was prolonged by 64 % in TG compared to corresponding WT cells (Fig. 5C). To study whether an altered localization of PP2A-B56α may have an impact on mitochondrial function either during ischemia or reperfusion, we measured the expression of B56α in mitochondrial preparations at different conditions. We found that the protein expression of B56α was increased after 30 min of reperfusion compared to basal conditions in TG hearts (Fig. 5D). The very low expression level of B56α in preparations of WT hearts allowed only a detection in TG. The protein expression of B56α was corrected to the voltage-dependent anion selective channel (VDAC), representing a marker for mitochondria.

3.5. Reduced fibrosis in TG hearts

To investigate whether the improved contractile function after ischemia-reperfusion in isolated hearts of transgenic mice is also reflected by corresponding changes in the intact animal, anesthetized WT and TG mice were subjected to transient LAD ligation for 120 min. After a 3-week recovery period, the formation of collagen fibers was quantified in heart sections stained with Heidenhain's AZAN trichrome. The collagen-rich fibrotic tissue is stained in blue (Fig. 6A). An attempt was always made to

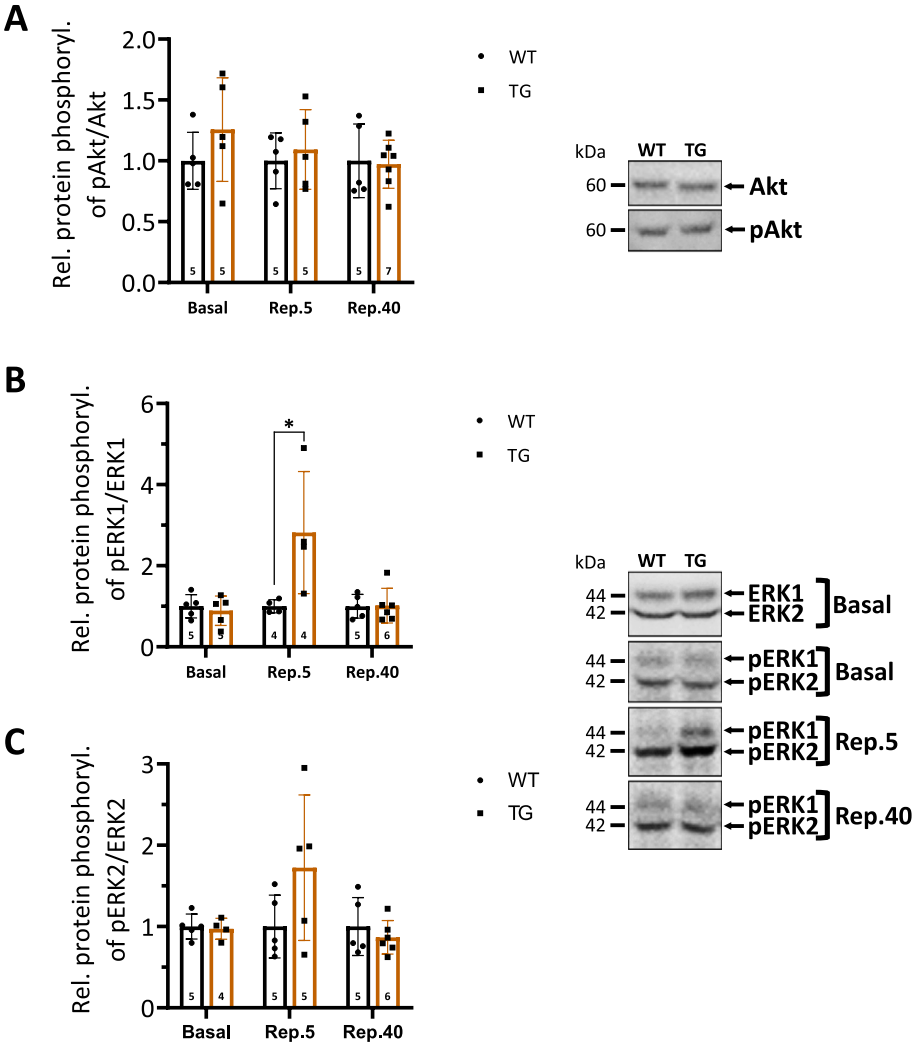

Fig. 4. Enhanced phosphorylation of ERK1 in TG hearts in early reperfusion. Isolated, Langendorff-perfused hearts were subjected to global ischemia and subsequent reperfusion. Thereafter, the expression of RISK phosphoproteins was determined under basal conditions and after early (5 min) and late (40 min) phases of reperfusion in heart homogenates. The summarized data are shown for relative phosphorylation of Akt (A), ERK1 (B) and ERK2 (C). The level of phosphorylation was related to the expression of the total protein. Representative immunoblots are depicted on the right-hand site (*$P < 0.05$ vs. WT; one-way ANOVA with Student-Newman-Keuls posttest; N = 4–7 hearts). More original examples of immunoblots are provided in Supplemental Fig. 2.

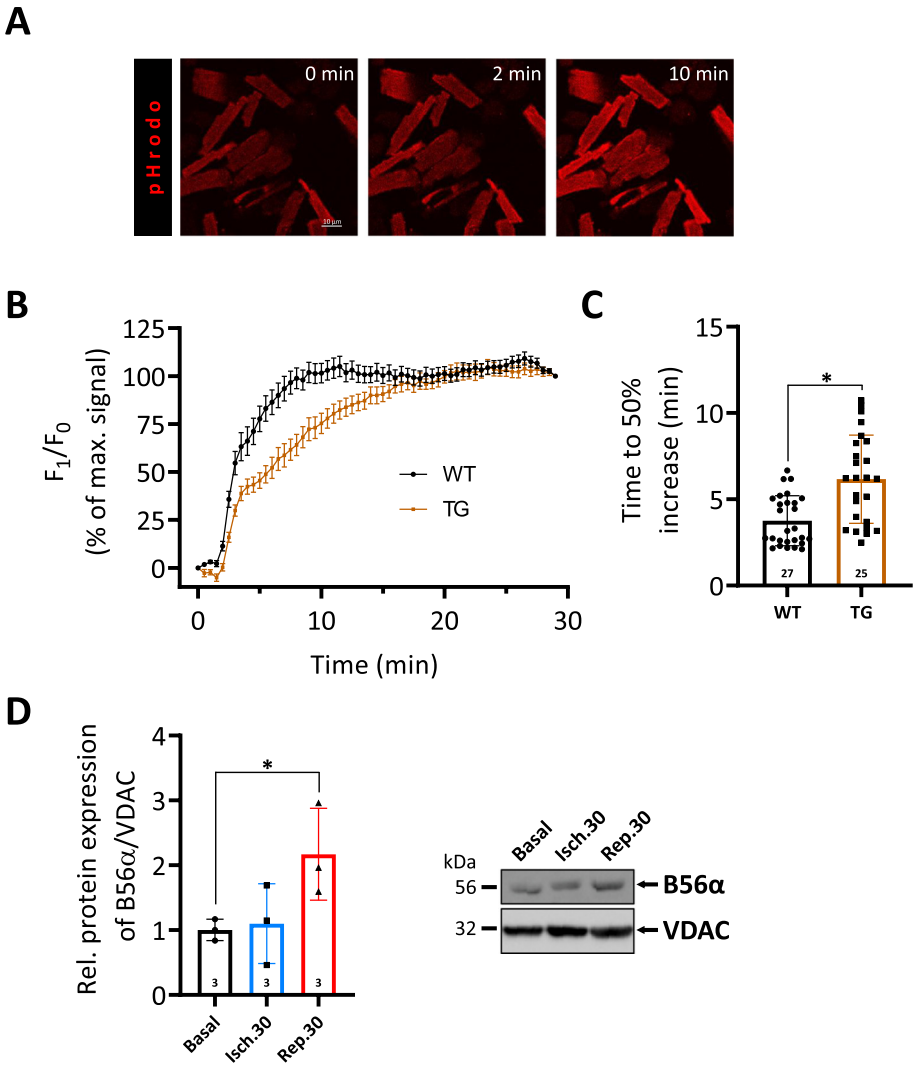

Fig. 5. Delayed development of acidosis in TG cardiomyocytes during ischemia. (A) Shown are representative images of isolated WT cardiomyocytes labeled with pHrodo Red (A). Cells were gassed with carbogen (5 % CO_2 and 95 % O_2) and the basal fluorescence signal was detected. Thereafter, cardiomyocytes were incubated with 20 % CO_2. A decrease in pH results in higher fluorescence intensities. The summarized data of percent increase of maximal fluorescence signal after incubation with 20 % CO_2 are given (B). The time to 50 % increase in F_1/F_0 signal was determined in both genotypes (C) (*$P < 0.05$ vs. WT; unpaired Student's *t*-test; n = 25–27 cardiomyocytes; N = 3 hearts each group). Mitochondrial preparations were obtained from isolated, Langendorff-perfused hearts subjected to a standard I/R protocol. The mitochondrial expression of B56α was measured under basal conditions, after a 30-min period of global ischemia and after 30 min of reperfusion. The summarized results are given (D, left panel) (*$P < 0.05$ vs. basal; one-way ANOVA with Student-Newman-Keuls posttest; N = 3 hearts each group). Representative immunoblots of B56α and the voltage-dependent anion channel, VDAC, which served as a reference protein, are depicted (D, right panel). Exhibiting very low expression levels in WT hearts, B56α could be only detected in mitochondrial preparations of TG hearts.

select the same cardiac cross-section for the following quantification of the degree of fibrosis representing the amount of fibrotic tissue in comparison to intact muscle tissue (in red). Here, we detected a reduced degree of fibrosis (by 53 %) in TG compared to corresponding WT hearts (Fig. 6B).

3.6. Identification of potential targets of PP2A-B56α after 40 min of reperfusion

To identify potential targets of PP2A-B56α that may explain the improved resistance against I/R injury, we performed 2D-differential gel electrophoresis with Pro-Q Diamond phosphoprotein staining followed by mass spectrometry-based protein analysis on heart samples that underwent 20 min of global ischemia with a subsequent 40-min-reperfusion phase (Fig. 7A) since contractile function was increased in TG vs. WT hearts at 40 min of reperfusion (Fig. 1). A fold value of 1.5 in protein spot staining intensity difference at $P \leq 0.05$ was set for the determination of significantly regulated proteins. In total, we identified 5 hyperphosphorylated and 28 hypophosphorylated proteins based on the response visualized by the phosphostain (for heatmap, see Fig. 7B); the spots of best quality were excised and analyzed (Table 1). This predominantly reduced phosphorylation of potential PP2A target proteins reflects well the increased PP2A activity after 40 min of reperfusion (Fig. 3E). Most of the detected proteins are located in the cytoplasm. However, we also found mitochondrial phosphoproteins representing potential targets of PP2A-B56α, which exhibited a higher expression in mitochondrial preparations of TG hearts after 30 min of reperfusion (Fig. 5D).

4. Discussion

Dysregulation of PP2A plays a key role in the development, progression, and severity of ischemia and I/R, but the exact mechanisms of its contribution remain poorly understood because it is not yet clear how regulatory B subunits can influence the phosphatase. However, this knowledge of the function of B subunits in the pathogenesis of I/R is necessary to utilize PP2A as a potential therapeutic target. In the heart, PP2Ac associates with

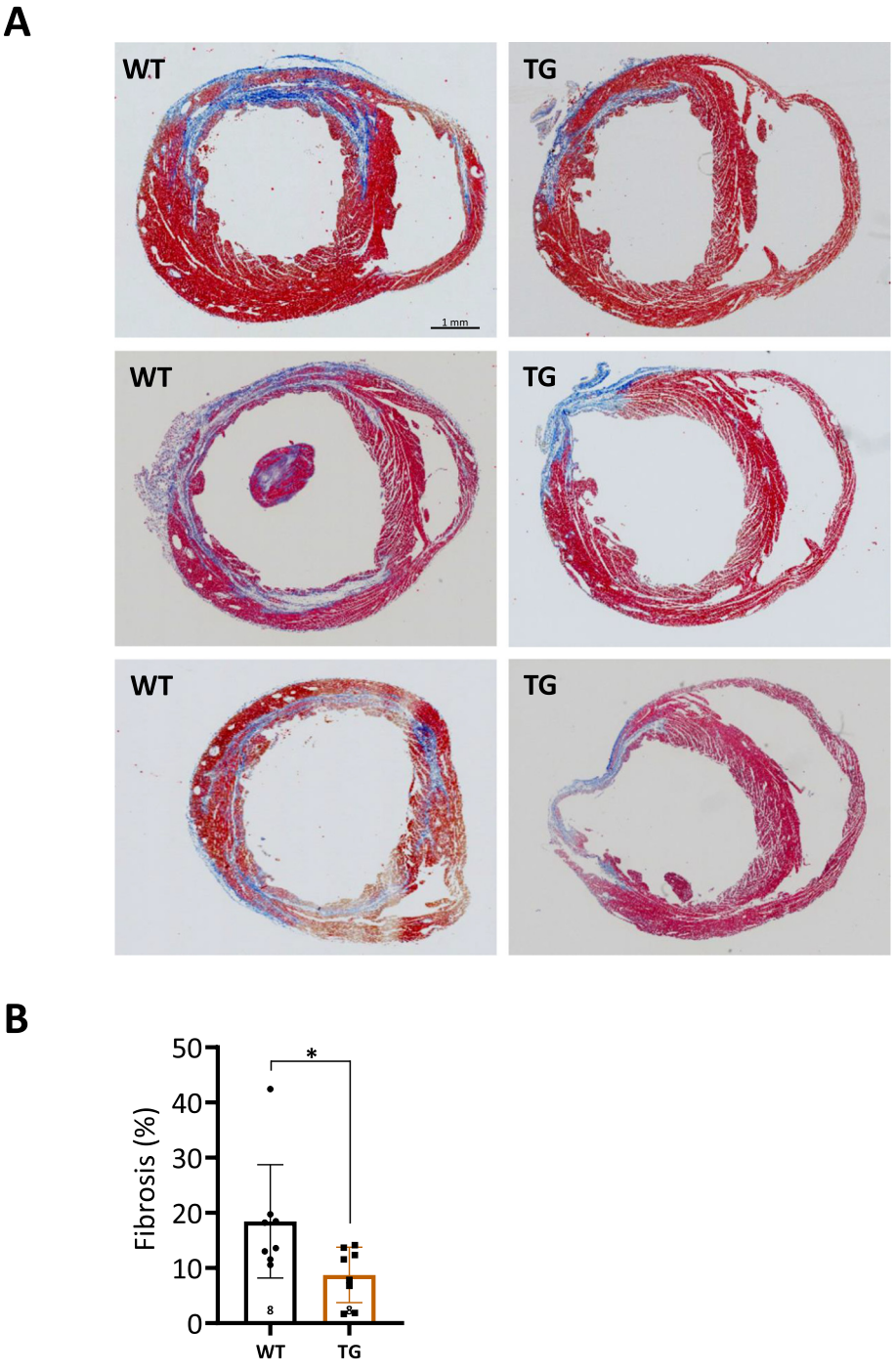

Fig. 6. Reduced fibrosis in heart sections of TG mice after coronary banding. Myocardial infarction was induced by 120 min ligation of the left anterior descending artery. Mice were killed 3 weeks after ligation by whole-body perfusion and fixation with paraformaldehyde (4 %). Hearts were excised, embedded in paraffin and then cut into 5-μm sections. Subsequently, sections were deparaffinized, rehydrated, and subjected to Heidenhain's AZAN trichrome staining which colorizes connective tissue such as the infarct scar deep blue, in contrast to the red cardiomyocytes of the remote heart tissue appearing brick-red. Representative sections of the same transverse heart level are shown for both genotypes (A). The amount of fibrotic area in percent of the whole heart section area was determined (B) (*$P < 0.05$ vs. WT; unpaired Student's *t*-test; N = 8 hearts each group).

over 40 specificity-determining B subunits that govern its local regulation by modulating subcellular localization and catalytic activity. Here, we demonstrate for the first time that direct cardiac-specific overexpression of the PP2Ac B′ subunit B56α increases contractile parameters in an isolated mouse heart model of I/R. Biochemical analyses demonstrated lower phosphorylation levels of MyBP-C and the RyR2 which was associated with higher PP2A activities in TG. The specificity of PP2A-B56α effects were confirmed by use of okadaic acid. The improved contractility in reperfused TG hearts was accompanied by a higher abundance of PP2A-B56α protein in mitochondrial preparations. We discovered that early reperfusion attenuated PP2A activity, thereby enhancing ERK1 phosphorylation in TG. We measured a prolonged ischemic contracture time in isolated TG hearts and a lower acidification in anoxic cardiomyocytes of TG hearts. Finally, we found that TG ventricles developed less fibrosis after transient LAD ligation and subsequent 3-week reperfusion.

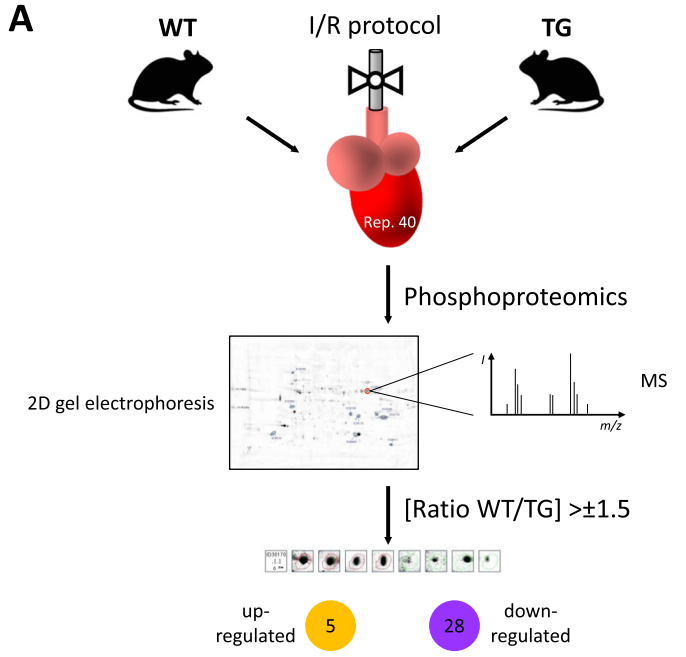

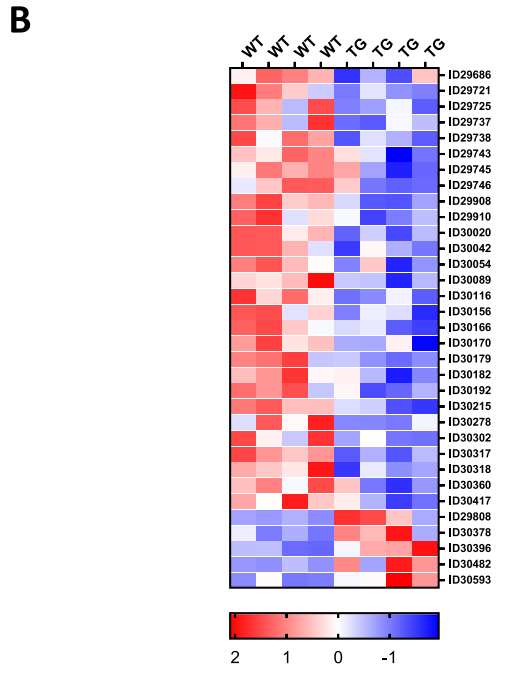

Fig. 7. Identification of potential PP2A-B56α targets under I/R conditions. Samples were taken from isolated Langendorff-perfused hearts of WT and TG mice after 40 min of reperfusion. After 2D-gel electrophoresis and ProQ Diamond staining, differentially regulated spots (showing a WT/TG ratio of $> \pm 1.5$, $P \leq 0.05$) where excised and analyzed by mass spectrometry (A). The individual phosphorylation levels of up- and downregulated proteins are represented by a heat map (B). A larger detailed image of the 2D gel with circled spots is shown in Supplemental Fig. 3. More details on the mass spectrometry analysis and Mascot engine search results are provided in Supplemental Table 1.

4.1. Regulation of PP2A catalytic activity by B56α during ischemia

The impact of changes in PP2A activity during ischemia and I/R remains controversial. In general, it seems to be consensus that during global ischemia, free radical-mediated oxidative cellular injury decreases activity and/or abundance of PP2A. In addition to the impairment of oxidative metabolism, hypoxia-inducible transcription factors (HIF) are also involved in the decrease of PP2A mRNA and expression [27]. Consistently, the administration of antioxidants attenuates the hypoxia-mediated attenuation of PP2A abundance [28,29]. The reduced abundance of PP2A could in turn directly affect the activity of the enzyme. This is contradicted, at least in part, by the decrease in activity observed in some studies without corresponding changes in protein expression [30,31], which may reflect an increased demethylation of PP2Ac, as occurs following prolonged intermittent hypoxia [32]. Alternatively, an increased phosphorylation of one of its regulatory subunits could be involved in the down-regulation of PP2A activity during ischemia. However, the kinase(s) responsible for phosphorylation of B subunits and subsequent inhibition of PP2A during ischemia remain(s) to be determined and we did not measure expression levels of phosphorylated B56α under I/R conditions. However, we demonstrated that under PKC-dependent phosphorylation of B56α at serine-41, PP2A activity decreases [19,33]. Although we have not yet directly measured PKC activity under conditions of ischemia, an increase has already been shown by other studies [34,35] and might explain the reduction of PP2A activity at the end of ischemia in our model. Thus, the prevention of a B subunit decrease observed by administration of antioxidants could contribute to the decrease in PP2A activity under 24 h of whole-organ-ischemia [28]. Unfortunately, these authors did not further specify which B subunit was detected. In line with this study, showing protective effects of a preserved expression of regulatory B subunits during ischemia, reduced PP2A-B55α contributed to an enlargement of the infarct size [36]. In contrast, short-term ischemia in a different cell culture model increased B56α expression levels [37]. Consistently, overexpression of PP2A-B56α was detrimental. Overall, discrepancies on the effects of individual regulatory subunits on PP2A activity suggest that the ischemia model used (i.e., analysis of samples at different time points), the expression level of the B subunits in different tissues (brain, kidney, or heart), and the specific signaling cascades activated play a role. The studies performed to date on this topic have only targeted the functional effects of ischemia on PP2A and its regulatory subunits. In the future, attempts should rather be made to stabilize the PP2A heterotrimer toward individual phospho-protein substrates by use of both specific genetically manipulated animal models of regulatory subunits or so-called small molecule PP2A activators, previously termed SMAPs [38].

4.2. PP2A-B56α-overexpressing mice resist against ischemic stress

The functional effects of B56α-mediated regulation of PP2A activity during the ischemic arrest of our I/R model were measured by determination of the time to 30 mm Hg of diastolic ventricular pressure. This parameter is a measure for the development of a so-called ischemic contracture, which is characterized by a firm, contracted left ventricle with obliteration of the ventricle cavity and blanching of the deeper layers of the myocardium [39]. The so-called “stone heart” has been attributed to the anaerobic depletion of energy stores leading to reduced ATP concentrations and strong linkages between actin and myosin [40]. The anaerobic generation of ATP in nonperfused hearts accumulates carbon dioxide and protons. Hence, we suggest that the increased time of ischemic contracture in TG, resulting in a weakened stiffness of the heart, is linked to the prolonged pH drop in TG cardiomyocytes under 20 % carbon dioxide (Fig. 8). Whether PP2A-B56α directly influences enzymes that are involved in lactate metabolism remains to be elucidated. However, it is conceivable that the lower acidification in TG may delay intracellular Ca^{2+} overload that is caused by aberrant ATP-dependent pump/exchanger ion activities [1]. A lower accumulation of Ca^{2+} might then contribute to the reduced degree of fibrosis after transient LAD occlusion in TG hearts. Changes in intracellular Ca^{2+} handling [41] have been implicated in the induction of myocardial hypertrophy and fibrosis, as observed 72 h after myocardial infarction [42]. Because calcium is the most dominant inducer of mitochondrial permeability transition pore (mPTP) opening [43], calcium overload would thus counteract the physiological closure of mPTPs during ischemia (Fig. 8). Mitochondrial Ca^{2+} influx in turn enhances proton leak and thus cytosolic acidification [44]. The prevention of Ca^{2+} overload would

Table 1

Here, we show potential target proteins of PP2A-B56α, differentially phosphorylated in B56α-TG vs. WT hearts under ischemia-reperfusion. Proteins were identified by mass spectrometry. More details on the mass spectrometry analysis and Mascot engine search results are provided in Supplemental Table 1.

Spot-ID	Protein	UniProt entry	Localization[a]	Function[a]	Phos.
30166	Glutathione S-transferase Mu 1	GSTM1_MOUSE	Cytoplasm	Glutathione conjugation	↓
29908	Phosphoglycerate kinase 1	PGK1_MOUSE	Cytoplasm	Glycolysis	↓
30318	60S acidic ribosomal protein P2	RLA2_MOUSE	Cytoplasm	Protein synthesis: elongation	↓
30156	Triosephosphate isomerase	TPIS_MOUSE	Cytoplasm	Glycolysis	↓
30482	Myoglobin	MYG_MOUSE	Cytoplasm, close to mitochondria	Oxygen storage	↑
30089	Myosin 6	MYH6_MOUSE	Filaments	Contraction	↓
29746	Myosin 7	MYH7_MOUSE	Myofilaments	Contraction	↓
30417	Cytochrome c oxidase subunit 6B1	CX6B1_MOUSE	Mitochondria	Electron transport chain	↓
30170	Glutamine amidotransferase-like class 1 domain-containing protein 3 (Gatd3, Gatd3a)	ES1_MOUSE	Mitochondria	Mitochondrial function	↓
30179	Cysteine and glycine-rich protein 3	CSRP3_MOUSE	Nucleus, cytoplasm, cytoskeleton, filaments	Mechano-signaling, calcium homeostasis, energy metabolism	↓

[a] Information was collected from UniProt database (www.uniprot.org); Phos. = extent of phosphorylation in TG vs. WT hearts, measured by ProQ-diamond staining after 2D-gel electrophoresis.

therefore contribute to the reduced apoptosis and fibrosis of cardiomyocytes [45], as observed in our LAD model.

4.3. Attenuation of PP2A activity leads to activation of ERK in TG hearts after ischemia

With the onset of reperfusion after the ischemic phase, oxidative phosphorylation is restored, leading to ATP production, pH correction, and reactivation of ion pumps. However, the O_2 burst also provides increased ROS production and cardiolipin oxidation, exacerbating dysfunction of electron transport chain [46]. Increased sarcolemmal Ca^{2+} influx and restoration of mitochondrial membrane potential drive Ca^{2+} into mitochondria, promoting mPTP opening and cytochrome *c* release. This leads to apoptosis and cardiomyocyte death. However, GSK-3β is also involved in the opening of mPTP during reperfusion [47]. In our study, the increase in ERK1 phosphorylation, which is associated with an attenuation of PP2A activity, leads to phosphorylation and inactivation of GSK-3β [48] and may contribute to the prevention of opening of mPTP and thus protection against reperfusion injury [47]. A link between increased ERK phosphorylation and decreased PP2A activity has also been described in other I/R models [49,50]. However, the mechanisms by which inactivation of GSK-3β leads to prevention of mPTP opening are still not fully understood. In any case, GSK3-3β has been identified as the integration point of many pathways (e.g., RISK) and transfers protective signals downstream to targets that act at the mPTP [51]. ERK-mediated phosphorylation of GSK-3β could abolish binding to ANT, resulting in a weakened interaction of ANT with CyPD, a trigger to close mPTP [51]. The translocation of PP2A-B56α in transgenic mitochondrial preparations 30 min after reperfusion may also contribute to a premature opening of mPTP. Cardiac arrest triggered translocation of PKC to mitochondria at 1 h reperfusion [52]. This was associated with inhibition of PP2A (probable via a member of the B′ family), inhibition of Bad dephosphorylation and a decrease in cytochrome *c* release. Whether an inhibition of Bcl-2 dephosphorylation by the mitochondrial PKC-phosphoB56α-PP2Ac signaling pathway contribute to anti-

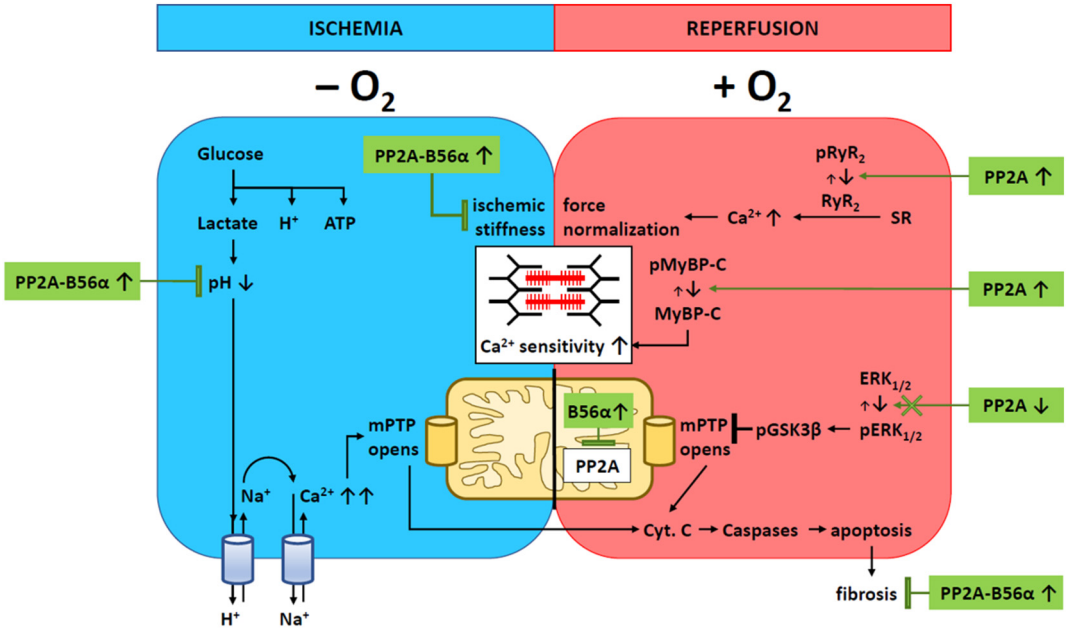

Fig. 8. Hypothesis of preservation of cardiac function in PP2A-B56α-overexpressing mice. During ischemia (-O_2) overexpression of PP2A-B56α prevents cardiac stiffness probably by an inhibition of myocellular Ca^{2+} overload and mPTP opening. The prolonged acidification in TG cardiomyocytes may contribute to this process leading to a decreased fibrosis in transiently LAD-ligated mice. During early reperfusion (+O_2) the B56α-mediated attenuation of PP2A activity might activate ERK1 resulting in inhibition of mPTP opening and cardioprotection. The translocation of B56α into mitochondria might help to inhibit PP2A, which suppresses the release of cytochrome *c*. At the late phase of reperfusion, higher PP2A activity was restored, which was paralleled by an increased contractility and lower okadaic acid-sensitive phosphorylation levels of MyBP-C and the RyR2.

apoptotic cardioprotective effects in our TG model remains to be elucidated. However, a role of PP2A-B56α as a regulator of the Bcl-2 family is likely [53].

4.4. Targeting of PP2A activity by B56α overexpression improves contractility during late reperfusion

The decrease in PP2A activity observed at the end of ischemia in our model was restored at the end of the reperfusion period. This finding supports our assumption of a direct regulation of PP2A activity by B56α when oxygen supply and cellular metabolism improve and the conditions for an inhibition of PP2A disappear. But how can the increase in PP2A activity be related to the higher contractility in isolated TG hearts? Previous studies detected a higher PP2A activity in the remote myocardium 24 h after 60 min LAD occlusion in mice that led to diminished phosphorylation of phospholamban at serine-16 and an impaired Ca^{2+} cycling [9]. The later may contribute to myocellular Ca^{2+} overload, a hallmark of I/R injury. Ca^{2+} overload was observed after ischemia and was suggested to result from a dysfunction of the sarcoplasmic reticulum (SR) complexome [54,55]. In contrast, antioxidant treatment attenuated Ca^{2+} overload [55]. The development of intracellular Ca^{2+} overload was also detected in reperfused rat hearts after 30 min of coronary artery occlusion [35]. However, this was linked to a PP1-dependent dephosphorylation of phospholamban. In our transgenic mouse model, the increased basal contractility was attributed to an enhanced myofilament Ca^{2+} sensitivity [20]. This, in turn, was related to a decrease in phosphorylation restricted to proteins of contractile myofilaments, whereas the phosphorylation of membrane-associated proteins was unaffected. We suggested a B56α-mediated targeting of PP2A to contractile relevant substrates. This effect might also occur in our present I/R model, where phosphorylated MyBP-C was reduced in TG after 40 min of reperfusion. The normalization of the phosphorylation level under application of okadaic acid indicates a PP2A-dependent process. Because PP2A is the main phosphatase controlling dephosphorylation of MyBP-C and loss of MyBP-C is associated with a higher Ca^{2+} sensitivity [56], we suggest that the decreased phosphorylation of MyBP-C contributes to the higher force development after reperfusion in TG (Fig. 8). Our data are in contrast to studies demonstrating that the phosphorylation level of MyBP-C is reduced after I/R injury, which was paralleled by increased cleavage of the protein, disruption of thick filaments, reduction in actomyosin cross-bridges and contractile impairment [57,58]. PP2A activity was not determined limiting the interpretation of the results. Whether the reduced phosphorylation of the RyR2 contributes to the improved contractility in reperfused TG hearts remains to be elucidated. However, exposure to myocytes to PP2Ac caused an immediate increase in Ca^{2+} spark frequencies followed by a depletion of SR Ca^{2+} stores [59]. The application of okadaic acid prevented these changes in SR Ca^{2+} cycling. Because PP2A co-localizes with the RyR2 [60] it is possible that B56α may also target PP2A to the junctional SR macromolecular complex during reperfusion leading to an enhanced SR Ca^{2+} release and contraction.

5. Limitations

Although showing overexpression of PP2A-B56α might protect against I/R injury, our study embodies some limitations. The three models we used, ex vivo ischemia-reperfusion hearts, in vivo LAD ligation mice and in vitro ischemic cardiomyocytes, approach the effects of PP2A-B56α overexpression on I/R very differently. Therefore, the comparability is limited, and conclusions must be handled carefully (Fig. 8). While contractile and biochemical characterization was carried out for 5 min and 40 min of reperfusion, 2D-gel electrophoresis with ProQ Diamond staining and mass spectrometry were undertaken only at 40 min of reperfusion (Fig. 7). It has not been elucidated how the potential target proteins, identified by mass spectrometry, are connected to the effects of PP2A-B56α overexpression. Moreover, ProQ-diamond staining is a well-established method for phosphoprotein identification, but a nonspecific staining can lead to false positive results. So, further investigation on the phosphoproteomic data is required (Fig. 7, Table 1). Under reperfusion, an increase of mitochondrial B56α levels was shown. But cytosolic B56α levels as well as mitochondrium associated PP2A activity were not measured and experiments were carried out only in TG hearts (Fig. 5). Further research is necessary to clarify the role of PP2A-B56α in mitochondria under I/R conditions.

6. Conclusions

Taken together, our results demonstrate that PP2A-B56α-overexpressing mice are protected against I/R injury which is associated with higher contractility, appropriate changes in the phosphorylation of Ca^{2+} regulatory proteins, and the activation of a cardioprotective signal transduction program. Moreover, transgenic mice resist against ischemic stress at the cellular level, in isolated Langendorff-perfused hearts and after transient LAD ligation in intact animals. We suggest that both substrate specificity and regulation of PP2Ac activity by B56α overexpression account for the cardioprotective effects in our mouse model. PP2A-B56α may represent an interesting therapeutic target in the pharmacological recruitment of myocardial salvage signaling in I/R.

Supplementary data to this article can be found online at https://doi.org/10.1016/j.jmccpl.2022.100030.

CRediT authorship contribution statement

Julius R. Herting: Formal analysis, Data curation, Writing – original draft, Writing – review & editing, Visualization. **Anna M. Berg:** Methodology, Software, Formal analysis, Investigation. **Katarina Hadova:** Methodology, Formal analysis, Investigation. **Alexander Heinick:** Methodology, Software, Formal analysis, Investigation, Visualization. **Simone König:** Methodology, Formal analysis, Investigation, Writing – review & editing. **Michael Kuhlmann:** Methodology, Investigation. **Frank U. Müller:** Resources, Supervision. **Uwe Kirchhefer:** Conceptualization, Validation, Resources, Data curation, Writing – original draft, Writing – review & editing, Visualization, Supervision, Project administration.

Declaration of competing interest

The authors declare that they have no known competing financial interests or personal relationships that could have appeared to influence the work reported in this paper.

Acknowledgments

We thank Nicole Hinsenhofen and Nina Goda for excellent technical assistance with the biochemistry experiments, John Eskander for his assistance in carrying out the Langendorff experiments, Melanie Voß for outstanding technical assistance with the isolation of ventricular cardiomyocytes, and Peter Boknik for his advice regarding protein phosphatase assays.

References

[1] Gottlieb RA. Cell death pathways in acute ischemia/reperfusion injury. J Cardiovasc Pharmacol Ther. 2011;16:233–8.
[2] Rodriguez-Sinovas A, Abdallah Y, Piper HM, Garcia-Dorado D. Reperfusion injury as a therapeutic challenge in patients with acute myocardial infarction. Heart Fail Rev. 2007;12:207–16.
[3] Kalogeris T, Baines CP, Krenz M, Korthuis RJ. Cell biology of ischemia/reperfusion injury. Int Rev Cell Mol Biol. 2012;298:229–317.
[4] Murphy E, Steenbergen C. Mechanisms underlying acute protection from cardiac ischemia-reperfusion injury. Physiol Rev. 2008;88:581–609.
[5] Garcia-Dorado D, Ruiz-Meana M, Inserte J, Rodriguez-Sinovas A, Piper HM. Calcium-mediated cell death during myocardial reperfusion. Cardiovasc Res. 2012;94:168–80.
[6] Armstrong SC, Ganote CE. Effects of the protein phosphatase inhibitors okadaic acid and calyculin A on metabolically inhibited and ischemic isolated myocytes. J Mol Cell Cardiol. 1992;24:869–84.
[7] Weinbrenner C, Baines CP, Liu GS, Armstrong SC, Ganote CE, Walsh AH, Honkanen RE, Cohen MV, Downey JM. Fostriecin, an inhibitor of protein phosphatase 2A, limits

myocardial infarct size even when administered after onset of ischemia. Circulation. 1998;98:899–905.
[8] Hoehn M, Zhang Y, Xu J, Gergs U, Boknik P, Werdan K, Neumann J, Ebelt H. Overexpression of protein phosphatase 2A in a murine model of chronic myocardial infarction leads to increased adverse remodeling but restores the regulation of β-catenin by glycogen synthase kinase 3β. Int J Cardiol. 2015;183:39–46.
[9] Kronenbitter A, Funk F, Hackert K, Gorreßen S, Glaser D, Boknik P, Poschmann G, Stühler K, Isic M, Krüger M, Schmitt JP. Impaired Ca2+ cycling of nonischemic myocytes contributes to sarcomere dysfunction early after myocardial infarction. J Mol Cell Cardiol. 2018;119:28–39.
[10] Szobi A, Lichy M, Carnicka S, Pancza D, Svec P, Ravingerova T, Adameova A. Pleiotropic effects of simvastatin on some calcium regulatory and myofibrillar proteins in ischemic/reperfused heart: causality of statins cardioprotection? Cur Pharm Des. 2016;22:6451–8.
[11] Xu Z, Kim S, Huh J. Zinc plays a critical role in the cardioprotective effect of postconditioning by enhancing the activation of the RISK pathway in rat hearts. J Mol Cell Cardiol. 2014;66:12–7.
[12] Penna C, Tullio F, Perrelli MG, Moro F, Abbadessa G, Piccione F, Carriero V, Racca S, Pagliaro P. Ischemia/reperfusion injury is increased and cardioprotection by a postconditioning protocol is lost as cardiac hypertrophy develops in nandrolone treated rats. Basic Res Cardiol. 2011;106:409–20.
[13] McCright B, Rivers AM, Audlin S, Virshup DM. The B56 family of protein phosphatase 2A (PP2A) regulatory subunits encodes differentiation-induced phosphoproteins that target PP2A to both nucleus and cytoplasm. J Biol Chem. 1996;271:22081–9.
[14] Price NE, Mumby MC. Effects of regulatory subunits on the kinetics of protein phosphatase 2A. Biochemistry. 2000;39:11312–8.
[15] Ito A, Koma Y, Sohda M, Watabe K, Nagano T, Misumi Y, Nojima H, Kitamura Y. Localization of the PP2A B56gamma regulatory subunit at the Golgi complex: possible role in vesicle transport and migration. Am J Pathol. 2003;162:479–89.
[16] Zhou XW, Mudannayake M, Green M, Gigena MS, Wang G, Shen RF, Rogers TB. Proteomic studies of PP2A-B56gamma1 phosphatase complexes reveal phosphorylation-regulated partners in cardiac local signaling. J Proteome Res. 2007;6:3433–42.
[17] McCright B, Virshup DM. Identification of a new family of protein phosphatase 2A regulatory subunits. J Biol Chem. 1995;270:26123–8.
[18] DeGrande ST, Little SC, Nixon DJ, Wright P, Snyder J, Dun W, Murphy N, Kilic A, Higgins R, Binkley PF, Boyden PA, Carnes CA, Anderson ME, Hund TJ, Mohler PJ. Molecular mechanisms underlying cardiac protein phosphatase 2A regulation in heart. J Biol Chem. 2013;288:1032–46.
[19] Kirchhefer U, Heinick A, König S, Kristensen T, Müller FU, Seidl MD, Boknik P. Protein phosphatase 2A is regulated by protein kinase Calpha (PKCalpha)-dependent phosphorylation of its targeting subunit B56alpha at Ser41. J Biol Chem. 2014;289:163–76.
[20] Kirchhefer U, Brekle C, Eskandar J, Isensee G, Kucerova D, Müller FU, Pinet F, Schulte JS, Seidl MD, Boknik P. Cardiac function is regulated by B56alpha-mediated targeting of protein phosphatase 2A (PP2A) to contractile relevant substrates. J Biol Chem. 2014;289:33862–73.
[21] Kucerova D, Baba HA, Boknik P, Fabritz L, Heinick A, Matus M, Müller FU, Neumann J, Schmitz W, Kirchhefer U. Modulation of SR Ca2+ release by the triadin-to-calsequestrin ratio in ventricular myocytes. Am J Physiol Heart Circ Physiol. 2012;302:H2008–17.
[22] Holmuhamedov EL, Jovanovic S, Dzeja PP, Jovanovic A, Terzic A. Mitochondrial ATP-sensitive K+ channels modulate cardiac mitochondrial function. Am J Physiol Heart Circ Physiol. 1998;275:H1567–76.
[23] Neumann J, Boknik P, Herzig S, Schmitz W, Scholz H, Gupta RC, Watanabe AM. Evidence for physiological functions of protein phosphatases in the heart: evaluation with okadaic acid. Am J Physiol Heart Circ Physiol. 1993;265:H257–66.
[24] Kirchhefer U, Baba HA, Kobayashi YM, Jones LR, Schmitz W, Neumann J. Altered function in atrium of transgenic mice overexpressing triadin 1. Am J Physiol Heart Circ Physiol. 2002;283:H1334–43.
[25] Kriegeskorte A, König S, Sander G, Pirkl A, Mahabir E, Proctor RA, von Eiff C, Peters G, Becker K. Small colony variants of Staphylococcus aureus reveal distinct protein profiles. Proteomics. 2011;11:2476–90.
[26] Kuhlmann MT, Kirchhof P, Klocke R, Hasib L, Stypmann J, Fabritz L, Stelljes M, Tian W, Zwiener M, Müller M, Kienast J, Breithardt G, Nikol S. G-CSF/SCF reduces inducible arrhythmias in the infarcted heart potentially via increased connexin43 expression and arteriogenesis. J Exp Med. 2006;203:87–97.
[27] Raghuraman G, Rai V, Peng Y-J, Prabhakar NR, Kumar GK. Pattern-specific sustained activation of tyrosine hydroxylase by intermittent hypoxia: role of reactive oxygen species-dependent downregulation of protein phosphatase 2A and upregulation of protein kinases. Antioxid RedoxSignal. 2009;11:1777–89.
[28] Koh PO. Ferulic acid attenuates the injury-induced decrease of protein phosphatase 2A subunit B in ischemic brain injury. PLoS One. 2013;8:e54217.
[29] Shah FA, Park DJ, Gim SA, Koh PO. Curcumin treatment recovery the decrease of protein phosphatase 2A subunit B induced by focal cerebral ischemia in Sprague-Dawley rats. Lab Anim Res. 2015;31:134–8.
[30] Hedou GF, Koshibu K, Farinelli M, Kilic E, Gee CE, Kilic U, Baumgärtel K, Hermann DM, Mansuy IM. Protein phosphatase 1-dependent bidirectional synaptic plasticity controls ischemic recovery in the adult brain. J Neurosci. 2008;28:154–62.
[31] Sung JH, Cho EH, Min W, Kim MJ, Kim MO, Jung EJ, Koh PO. Identification of proteins regulated by estradiol in focal cerebral ischemic injury–a proteomics approach. Neurosci Lett. 2010;477:66–71.
[32] Zhang CE, Yang X, Li L, Sui X, Tian Q, Wei W, Wang J, Liu G. Hypoxia-induced tau phosphorylation and memory deficit in rats. Neurodegener Dis. 2014;14:107–16.
[33] Pluteanu F, Boknik P, Heinick A, König C, Müller FU, Weidlich A, Kirchhefer U. Activation of PKC results in improved contractile effects and Ca2+ cycling by inhibition of PP2A-B56α. Am J Physiol Heart Circ Physiol. 2022;322:H427–41.
[34] Armstrong SC. Protein kinase activation and myocardial ischemia/reperfusion injury. Cardiovasc Res. 2004;61:427–36.
[35] Shintani-Ishida K, Yoshida K. Ischemia induces phospholamban dephosphorylation via activation of calcineurin, PKC-α, and protein phosphatase 1, thereby inducing calcium overload in reperfusion. Biochim Biophys Acta. 2011;1812:743–51.
[36] Tobisawa T, Yano T, Tanno M, Miki T, Kuno A, Kimura Y, Ishikawa S, Kouzu H, Nishizawa K, Yoshida H, Miura T. Insufficient activation of Akt upon reperfusion because of its novel modification by reduced PP2A-B55α contributes to enlargement of infarct size by chronic kidney disease. Basic Res Cardiol. 2017;112:31.
[37] Tsao CC, Nica AF, Kurinna SM, Jiffar T, Mumby M, Ruvolo PP. Mitochondrial protein phosphatase 2A regulates cell death induced by simulated ischemia in kidney NRK-52E cells. Cell Cycle. 2007;6:2377–85.
[38] Leonard D, Huang W, Izadmehr S, O'Connor CM, Wiredja DD, Wang Z, Zaware N, Chen Y, Schlatzer DM, Kiselar J, Vasireddi N, Schüchner S, Perl AL, Galsky MD, Xu W, Brautigan DL, Ogris E, Taylor DJ, Narla G. Selective PP2A enhancement through biased heterotrimer stabilization. Cell. 2020;181:688–701.
[39] Cooley DA, Reul GJ, Wukasch DC. Ischemic contracture of the heart: "Stone heart". Am J Cardiol. 1972;29:575–7.
[40] Katz AM, Tada M. The „stone heart": a challenge to the biochemist. Am J Cardiol. 1972;29:578–80.
[41] Lips DJ, deWindt LJ, van Kraaij DJ, Doevendans PA. Molecular determinants of myocardial hypertrophy and failure: alternative pathways for beneficial and maladaptive hypertrophy. Eur Heart J. 2003;24:883–96.
[42] Tsuda T, Gao E, Evangelisti L, Markova D, Ma X, Chu ML. Post-ischemic myocardial fibrosis occurs independent of hemodynamic changes. Cardiovasc Res. 2003;59:926–33.
[43] Halestrap AP, Richardson AP. The mitochondrial permeability transition: a current perspective on its identity and role in ischaemia/reperfusion injury. J Mol Cell Cardiol. 2015;78:129–41.
[44] Nanayakkara GK, Wang H, Yang X. Proton leak regulates mitochondrial reactive oxygen species generation in endothelial cell activation and inflammation - a novel concept. Arch Biochem Biophys. 2019;662:68–74.
[45] Hausenloy DJ, Yellon DM. The mitochondrial permeability transition pore: its fundamental role in mediating cell death during ischemia and reperfusion. J Mol Cell Cardiol. 2003;35:339–41.
[46] Paradies G, Paradies V, Ruggiero FM, Petrosillo G. Mitochondrial bioenergetics and cardiolipin alterations in myocardial ischemia-reperfusion injury: implications for pharmacological cardioprotection. Am J Physiol Heart Circ Physiol. 2018;315:H1341–52.
[47] Miura T, Tanno M. Mitochondria and GSK-3β in cardioprotection against ischemia/reperfusion injury. Cardiovasc Drugs Ther. 2010;24:255–63.
[48] Heusch G. Molecular basis of cardioprotection: signal transduction in ischemic pre-, post-, and remote conditioning. Circ Res. 2015;116:674–99.
[49] Martín de la Vega C, Burda J, Toledo Lobo MV, Salinas M. Cerebral postischemic reperfusion-induced demethylation of the protein phosphatase 2A catalytic subunit. J Neurosci Res. 2002;69:540–9.
[50] Hu X, Wu X, Xu J, Zhou J, Han X, Guo J. Src kinase up-regulates the ERK cascade through inactivation of protein phosphatase 2A following cerebral ischemia. BMC Neurosci. 2009;10:74.
[51] Juhaszova M, Zorov DB, Yaniv Y, Nuss HB, Wang S, Sollott SJ. Role of glycogen synthase kinase-3beta in cardioprotection. Circ Res. 2009;104:1240–52.
[52] Dave KR, Bhattacharya SK, Saul I, DeFazio RA, Dezfulian C, Lin HW, Raval AP, Perez-Pinzon MA. Activation of protein kinase C delta following cerebral ischemia leads to release of cytochrome C from the mitochondria via bad pathway. PLoS One. 2011;6:e22057.
[53] Van Hoof C, Goris J. Phosphatases in apoptosis: to be or not to be, PP2A is in the heart of the question. Biochim Biophys Acta. 2003;1640:97–104.
[54] Valverde CA, Mundiña-Weilenmann C, Reyes M, Kranias EG, Escobar AL, Mattiazzi A. Phospholamban phosphorylation sites enhance the recovery of intracellular Ca2+ after perfusion arrest in isolated, perfused mouse heart. Cardiovasc Res. 2006;70:335–45.
[55] Saini HK, Dhalla NS. Defective calcium handling in cardiomyocytes isolated from hearts subjected to ischemia-reperfusion. Am J Physiol Heart Circ Physiol. 2005;288:H2260–70.
[56] Cazorla O, Szilagyi S, Vignier N, Salazar G, Krämer E, Vassort G, Carrier L, Lacampagne A. Length and protein kinase A modulations of myocytes in cardiac myosin binding protein C-deficient mice. Cardiovasc Res. 2006;69:370–80.
[57] Decker RS, Decker ML, Kulikovskaya I, Nakamura S, Lee DC, Harris K, Klocke FJ, Winegrad S. Myosin-binding protein C phosphorylation, myofibril structure, and contractile function during low-flow ischemia. Circulation. 2005;111:906–12.
[58] Sadayappan S, Osinska H, Klevitsky R, Lorenz JN, Sargent M, Molkentin JD, Seidman CE, Seidman JG, Robbins J. Cardiac myosin binding protein C phosphorylation is cardioprotective. Proc Natl Acad Sci USA. 2006;103:16918–23.
[59] Terentyev D, Viatchenko-Karpinski S, Gyorke I, Terentyeva R, Gyorke S. Protein phosphatases decrease sarcoplasmic reticulum calcium content by stimulating calcium release in cardiac myocytes. J Physiol. 2003;552:109–18.
[60] Alsina KM, Hulsurkar M, Brandenburg S, Kownatzki-Danger D, Lenz C, Urlaub H, et al. Loss of protein phosphatase 1 regulatory subunit PPP1R3A promotes atrial fibrillation. Circulation. 2019;140:681–93.